

Spin textures in strongly coupled electron spin and magnetic or nuclear spin systems in quantum dots

Ramin M. Abolfath^{1,2,3}, Marek Korkusinski³, Thomas Brabec², Pawel Hawrylak^{2,3}

¹*School of Natural Sciences and Mathematics, University of Texas at Dallas, Richardson, TX 75080*

²*University of Ottawa, Physics Department 150 Louis Pasteur, Ottawa, ON, K1N 6N5, Canada*

³*Institute for Microstructural Sciences, National Research Council of Canada, Ottawa, K1A 0R6*

(Dated: December 3, 2024)

Controlling electron spins strongly coupled to magnetic and nuclear spins in solid state systems is an important challenge in the field of spintronics and quantum computation. We show here that electron droplets with no net spin in semiconductor quantum dots strongly coupled with magnetic ion/nuclear spin systems break down at low temperature and form a non-trivial anti-ferromagnetic spatially ordered spin-texture of magneto-polarons. The spatially ordered combined electron-magnetic ion spin-texture, associated with spontaneous symmetry-breaking in the parity of electronic charge density and magnetization of magnetic ions, emerge from both ab-initio density functional approach to the electronic system coupled with mean-field approximation for the magnetic/nuclear spin system and fully microscopic exact diagonalization of small systems. The predicted phase diagram determines the critical temperature as a function of coupling strength and identifies possible phases of the strongly coupled spin system. This prediction may arrest fluctuations in spin system and open the way to control, manipulate and prepare magnetic and nuclear spin ensembles in semiconductor nanostructures.

PACS numbers: 81.07.Ta, 75.75.Fk

There is currently significant interest in developing quantum information storage and processing capabilities [1] using electron spins strongly coupled to spins of either magnetic ions (MI) or/and nuclei (NS) in a number of solid state systems. This includes GaAs based gated two-dimensional [2] and zero-dimensional systems [3–5], InAs self-assembled quantum dots [6–8], CdTe quantum dots [9–21], nanocrystals [22], NV centers in diamond [23], phosphor impurities in silicon [24] and carbon nanotubes [25].

In these systems electron spins play either a role of qubits or are used to control magnetic or nuclear spins. For electron spin qubits much effort went recently to determine the role of decoherence by nuclear spins [4, 5]. For electrons interacting with magnetic ions in diluted magnetic semiconductors, the central spin problem has been understood in terms of magnetic polarons - a cloud of magnetization surrounding a localized electron spin [26]. On the other hand, the interaction of many electrons in a spin singlet state in, e.g., a metal [27] or a quantum dot [14, 15] induces RKKY interaction among nuclear and/or magnetic ion spins. The question of whether spin textures could form in a strongly coupled two-dimensional electron gas-nuclear spin subsystem has been addressed recently by Loss *et al.* [28]. Both scenarios of magnetic polarons and RKKY interactions can be realized in semiconductor quantum dots containing magnetic ions and/or nuclear spins by changing electron concentration with a gate, through modulation doping [14, 15] or through deformation of quantum dot confining potential [17]. Spin singlet droplets are already employed in initialization of coded qubits in lateral quantum dots [3] and as component of trions in

optical manipulation of spin in self-assembled quantum dots [7, 8].

In this work, we use both ab-initio density functional approach to the electronic system and mean-field approximation for the magnetic/nuclear spin system and exact diagonalization of the fully microscopic Hamiltonian of electron-magnetic ion interacting system to show that beyond RKKY approximation spin singlet electron droplet corresponding to closed-shell quantum dots strongly coupled with magnetic ion/nuclear spin systems breaks down and forms a non-trivial anti-ferromagnetic spatially ordered spin-texture of magneto-polarons at low temperature. This prediction opens the way to control, manipulate and prepare magnetic and nuclear spin ensembles in semiconductor nanostructures.

We focus here on closed-shell QDs [29] containing $N = 2, 6, 12, \dots$ electrons in the presence of many spins of either magnetic ions, e.g., mangan in CdTe [14, 15, 26, 30] or nuclear spins. We approximate many spins by a continuous magnetization [16, 17] and study the strongly coupled electronic-magnetic system as a function of temperature T , number of electrons N , strength of exchange coupling J_{sd} , magnetic ion density n_m and strength of confining potential ω_0 .

In particular, we find that for a given confining potential and magnetic ion density, there exists a critical temperature, T^* for a two-dimensional nucleation and growth of inhomogeneous AFM spin-textures with broken symmetry. Below T^* and above a critical electron-magnetic ion spin coupling strength, spin singlet droplet and a homogeneous magnetization density breaks down and molecular states of magnetic polarons associated with individual electron spins form. The magneto-

polarens correspond to the inhomogeneous magnetic field of MI's inducing an effective spatially varying potential localizing electrons with spin up in different positions from the electrons with spin down, significantly changing electronic charge distribution.

This is to be compared with closed-shell QDs with large confinement potential and with only two MI's [14, 15]. Using exact diagonalization of the interacting electron-electron and electron-MI Hamiltonian it has been shown that the RKKY coupling, a second-order effective interaction between MI's, describes well the ground state with total magnetic moment $M_z = 0$ (AFM-ordering) and $M_z = 2M$ (FM-ordering) depending on the relative position of MI's in a QD, while maintaining the spin singlet electronic ground state with dipole moment $P_z = 0$. A related problem has been recently studied where an analytical variational form of the two-electrons wavefunction coupled to a large number of MI, neither two-body singlet nor triplet, called pseudo-singlet, was introduced to describe partial quantum correlations of the coupled spin singlet-MI system [21].

We use both ab-initio density functional to describe the droplet of electrons in a parabolic quantum dot with closed electronic shells for $N = 2, 6, 12, \dots$ electrons and mean-field approximation for the magnetic/nuclear spin system [16] and a fully microscopic approach to interacting electron-magnetic ion system but limited to smaller systems [12]. In ab-initio DFT we employ spin unrestricted local density approximation (LSDA) for electrons where the many-body Hamiltonian is replaced by the Kohn-Sham (KS) Hamiltonian, H_{KS} . In LSDA, the self-consistent KS orbitals are calculated for spin up and down independently, without any additional symmetrization of their spatial dependence. The electrons interact with a magnetic field produced by the magnetic ions which in turn is determined self-consistently by the spin density of the electronic system, with details described in the Methods section and in Refs. 16, 17.

The spatial dependence of the z -component of magnetization $M_z(\vec{r})$ of Mn ions, solutions of the self-consistent LSDA equations for the coupled electronic-magnetic ion system, are shown in Fig. 1(a-c) for closed shell parabolic QD corresponding to $\omega_0 = 2Ry^*$, $n_m = 0.1 \text{ nm}^{-3}$ and temperature $T = 0.5 \text{ K}$ for $N = 2$, Fig. 1(a), $N = 6$ Fig. 1(b) and $N = 12$, Fig. 1(c). Note that the total magnetization per unit area A , $\langle M_z \rangle = \frac{1}{A} \int d^2r \langle M_z(\vec{r}) \rangle = 0$, indicating net AFM ordering in the ground state of MIs. These states clearly resemble spin texture with broken rotational symmetry. By inspection we see two spatially separated magnetization clouds for a two electron quantum dot, six for six electrons, and twelve for twelve electrons. Hence we consider these states as molecules of magneto-polarons. The inset shows schematically electron spin density for twelve electrons with a decagon ring structure and two electrons in the middle in form of spin-corrals, a circular symmetric spin texture (see Fig. 3).

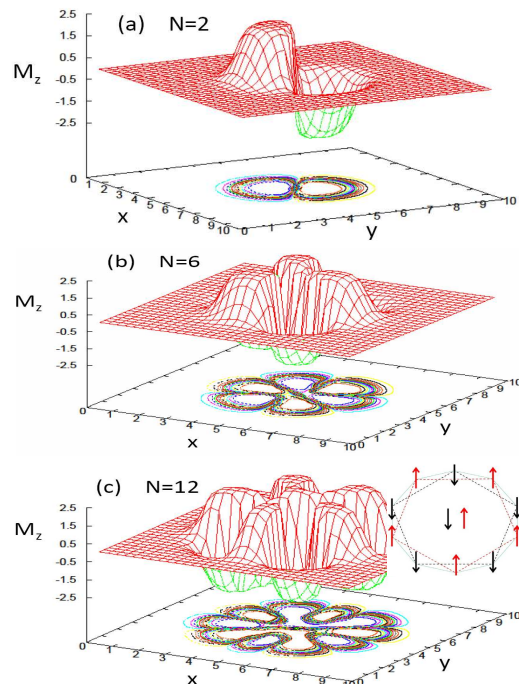


FIG. 1: The spatial profile of Mn-magnetization for a closed shell parabolic QD with $\omega_0 = 2Ry^*$ and $n_m = 0.1 \text{ nm}^{-3}$. (a), (b), and (c) correspond to $N = 2, 6, 12$ at $T = 0.5 \text{ K}$ and $J_{sd} = 15 \text{ meV nm}^{-3}$. Coordinates (x, y) are expressed in effective Bohr radius. Inset in Fig.1c shows a decagon molecular structure of $N = 12$ closed-shell QD with a molecular state of 12 magnetic polarons, each shown by an arrow. The direction of arrows show the direction of M_z in each magnetic polaron.

The inhomogeneous spin density gives way to a uniform solution in which $M_z = s_z = 0$ for $T > T^* \approx 2 \text{ K}$ independent of N and ω_0 . Note that this finding is in contrast with open shell FM states that are stable up to $T \approx 20 \text{ K}$ [16, 17] and the FM state proposed recently in Ref. [21] for closed-shell QDs.

To investigate the origin and stability of AFM states presented in this work, we focus on a closed-shell QD with $N = 2$. Let us first consider the RKKY interaction between two magnetic ions at positions $\vec{R}_1 = (X, 0)$ and $\vec{R}_2 = (-X, 0)$: $J(X) = -\gamma(2 - 5X^2)e^{-X^2}$, where $\gamma = (J^{2D}/\pi l_0)^2 \times (1/(16\omega_0))$ and distance is measured in l_0 [14]. We see that for $X > \sqrt{2/5}$ the interaction is AFM. It is now possible to imagine that the RKKY interaction triggers a broken symmetry state where the exchange interaction localizes an electron with spin up on the left magnetic ion and spin down electron on the right magnetic ion. This conclusion is supported both by the exact diagonalization of the Hamiltonian of $N = 2$ electrons interacting with two magnetic ions and from

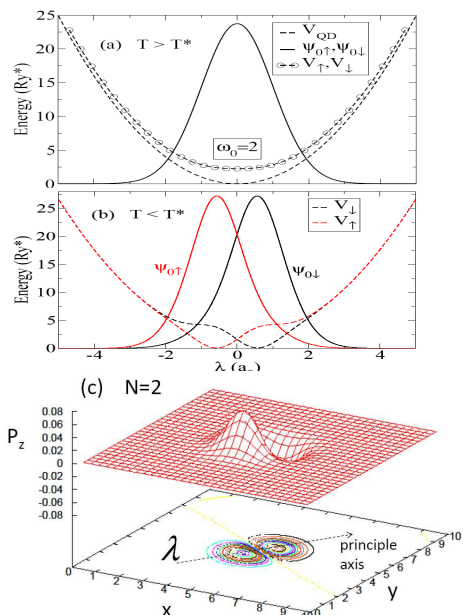


FIG. 2: The spatial profile of spin-dependent electron wave-functions in a closed shell parabolic QD with $N = 2$, $\omega_0 = 2Ry^*$, $n_m = 0.1\text{nm}^{-3}$. In (a) $T > T^*$, $M_z = P_z = 0$ and $\psi_{0\uparrow} = \psi_{0\downarrow}$. The dashed lines show the QD parabolic confining potential, V_{QD} . The spin-dependent effective potential $V_\sigma = V_{\text{QD}} + V_H + V_{XC}^\sigma - \sigma h_{sd}/2$ is shown by dashed lines with open circles in which $V_\uparrow = V_\downarrow$ for $T > T^*$. In (b) $T < T^*$. A pronounced displacement in spin-dependent wave-functions is visible, an indication in spatial phase separation of spin up and down electrons that led to the two-dimensional profile of electron spin-polarization shown in (c). $P_z = (n_\uparrow - n_\downarrow)/2$. Two asymmetric bumps in effective potentials V_\uparrow and V_\downarrow are a result of inhomogeneous magnetic field of MI's. In (b) the bottom of potentials V_\uparrow and V_\downarrow are shifted to zero. The horizontal-axis used in (a) and (b) is plotted along the diagonal-direction of P_z shown as principle axis by a dashed-arrow in (c), and denoted by λ in (b). Along this direction the difference between V_\uparrow and V_\downarrow is maximum. Planar coordinates (x, y) are expressed in effective Bohr radius (a_0).

the self-consistent solutions of LSDA equations.

In Figs. 2 we show self-consistent solutions of LSDA equations including the effective potential V_σ and spatial profile of spin-dependent KS wave-functions for parabolic confining potential with level spacing $\omega_0 = 2Ry^*$. In Fig. 2(a), $T = 2\text{K}$ and the paramagnetic state with $M_z = P_z = 0$ is the ground state. The spin-dependent effective potential V_σ is shown with open-circles in which $V_\uparrow = V_\downarrow$. In this case we find that the self-consistent KS eigen-energies and eigen-states with opposite spins are identical, $\epsilon_{0\uparrow} = \epsilon_{0\downarrow}$ and $\psi_{0\uparrow} = \psi_{0\downarrow}$.

In Fig. 2(b) we present our results for $T = 0.5\text{K}$. Interestingly, with decreasing temperature a continuous

displacement in spin-dependent wave-functions develops that spontaneously breaks the circular symmetry of the QD as discussed above. In this case we find two degenerate spatially separated wavefunctions $\psi_{0\uparrow}$ and $\psi_{0\downarrow}$ with $\epsilon_{0\uparrow} = \epsilon_{0\downarrow}$. This is analogous to the nucleation of para- H_2 molecule from para-He if two nuclei of He undergo a continuous fragmentation. A two-dimensional profile of electron spin-polarization $P_z = (n_\uparrow - n_\downarrow)/2$ shown in (c) is also a result of spontaneous spatial spin-separation of KS orbitals.

Two asymmetric bumps observed in effective potentials V_\uparrow and V_\downarrow are the result of spontaneous formation of AFM spin texture in M_z . In effective potential, V_σ , both exchange-correlation potential V_{XC}^σ and h_{sd} show dependence on M_z . By definition, $h_{sd} = J_{sd}M_z/M$ linearly depends on M_z . Although V_{XC}^σ is a non-linear function of M_z , we find $V_{XC}^\downarrow - V_{XC}^\uparrow = cM_z$, where c is a constant. Hence $V_\downarrow - V_\uparrow = V_{XC}^\downarrow - V_{XC}^\uparrow + h_{sd} = (c + J_{sd}/M)M_z$, i.e., it scales linearly with M_z . Defining λ , a coordinate variable along the principle axis of $P_z = (n_\uparrow - n_\downarrow)/2$ shown by a dashed-arrow in Fig. 2(c), we find that $f(\lambda) = a\lambda \exp(-b\lambda^2)$ numerically fits M_z with a and b as fitting parameters. This indicates that M_z is odd under parity transformation ($\lambda \rightarrow -\lambda$).

The spontaneous symmetry breaking and the formation of magnetic polarons depends on the parameters of the system. For example, in the example studied here, the critical temperature depends on electron spin-magnetic ion coupling strength $J_{em} = J_{sd}n_mM$, which is proportional to exchange coupling, magnetic ion density and magnetic ion spin. Figure 3 shows the phase diagram of $N = 2$ closed shell QD with $\omega_0 = 2Ry^*$ and $n_m = 0.1\text{nm}^{-3}$. The curves show critical temperature as a function of J_{em} . In the limit of low J_{em} , e.g., either for electrons and/or low density of magnetic ions, a direct transition from AFM spin texture, shown as inset, to normal state is seen. For high J_{em} , e.g., for either holes and/or high density of magnetic ions, a transition through an intermediate state of spin-corral, shown as inset (see Fig. 3) is observed. This is a transition from rotational symmetry breaking state, stable at low temperatures, to another type of spin texture with rotational symmetry, stable within $T_1^* \leq T \leq T_2^*$. For $J_{sd} = 75\text{meV nm}^{-3}$ and $n_m = 0.1$ we find $T_1^* = 17$ and $T_2^* = 35\text{K}$.

To summarize, low temperature solutions of ab-initio density functional approach to electrons in closed-shell quantum dots strongly coupled with the magnetic/nuclear spin system described in the mean-field approximation and fully microscopic theory for small systems show that the local symmetry of spin singlet state spontaneously breaks down and forms geometrically ordered molecules of single magnetic polarons. The phase diagram of topologically stable non-trivial antiferromagnetically ordered and spin-corral states determined by the number of electrons in a quantum dot, magnetic

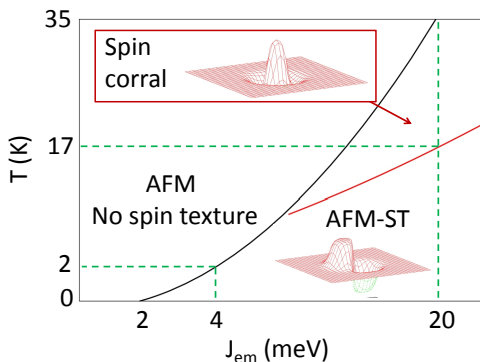


FIG. 3: Phase diagram, temperature T vs electronic-magnetic ion coupling strength J_{em} of $N = 2$ closed-shell QD with $\omega_0 = 2Ry^*$.

ion density, exchange coupling strength, temperature and confining potential. This prediction may arrest fluctuations in spin system and open the way to control, manipulate and prepare magnetic and nuclear spin ensembles in semiconductor nanostructures for quantum information processing and storage.

Methods: In this work, we use both ab-initio density functional approach to the electronic system and mean-field approximation for the magnetic/nuclear spin system and fully microscopic theory described in detail in Ref. [14]. In ab-initio approach we employ spin unrestricted local density approximation (LSDA) for electrons where the many-body Hamiltonian is replaced by the Kohn-Sham (KS) Hamiltonian, H_{KS} . In LSDA, the self-consistent KS orbitals are calculated for spin up and down independently, without any additional symmetrization of their spatial dependence. Electrons (more rigorously quasi-particles) fill KS-orbitals according to Fermi statistics at finite temperature and the electronic correlations are taken into account via exchange-correlation (XC) energy functional. In this approach, the self-consistent solutions form a large class of variational many-body wave-functions, among them the configuration with the lowest free-energy is found that represents the ground state at finite temperature T . We also decompose the planar and perpendicular components of the confining potential of a single QD as described in Ref. [16, 17] and expand the electron wavefunctions in terms of its planar $\psi_{i\sigma}(\vec{r})$, and subband wave function $\xi(z)$, and project H_{KS} onto the XY-plane by integrating out $\xi(z)$, assuming that only the lowest energy subband is filled. Hence KS orbitals, $\psi_{i\sigma}(\vec{r})$, are calculated by diagonalizing $H_{KS}\psi_{i\sigma}(\vec{r}) = \epsilon_{i\sigma}\psi_{i\sigma}(\vec{r})$, in real-space. Here $\epsilon_{i\sigma}$ is the KS eigen-energies, and $H_{KS} = \frac{-\hbar^2}{2m^*}\nabla_r^2 + V_\sigma$ with KS effective potential denoted as $V_\sigma = V_{QD} + V_H +$

$V_{XC}^\sigma - \frac{\sigma}{2}\hbar s_d(\vec{r})$. \hbar is the Planck constant, m^* is the electron effective mass, $-e$ is the electron charge and $\sigma = \pm 1$ denotes spin up (\uparrow) and down (\downarrow). V_{QD} is the planar confining potential of QD, V_H and V_{XC}^σ are Hartree and spin dependent exchange-correlation potentials and $h_{sd}(\vec{r}) = J_{em} \int dz |\xi(z)|^2 B_M(Mb(\vec{r}, z)/k_B T)$. $J_{em} = J_{sd} n_m M$ is the mean-field e-Mn exchange coupling, J_{sd} is the local exchange coupling between electron spin and magnetic-impurity/nuclear spins with average density n_m . The direct Mn-Mn antiferromagnetic coupling is negligible in the range of MI densities considered in this study. Here $B_M(x)$ is the Brillouin function [30], k_B is the Boltzmann constant, and $b(\mathbf{r}_i) = J_{sd}[n_\uparrow(\mathbf{r}_i) - n_\downarrow(\mathbf{r}_i)]/2$ is the effective field seen by Mn ions.

For strongly coupled electronic-magnetic ion system we perform numerical calculation for (Cd,Mn)Te where $a_B^* = 5.29$ nm, and $Ry^* = 12.8$ meV are the effective Bohr radius and Rydberg, the sd exchange coupling is $J_{sd} = 0.015$ eV nm³, effective mass $m^* = 0.106$, and $\epsilon = 10.6$ [12]. We consider QD's with confining ω_0 in the range of $1 - 3Ry^*$, the perpendicular width of 1 nm, and a variable magnetic ion density n_m . For definiteness, we focus on the example of Mn isoelectronic impurity in CdTe, with the z -component of \vec{M}_I of impurity spin satisfying $M_z = -M, -M + 1, \dots, M$ and $M = 5/2$.

Acknowledgement: The authors thank the NSERC, QuantumWorks and CIFAR for support.

-
- [1] *Semiconductor quantum bits*, World Scientific, 2008; O. Benson and F. Henneberger, Editors.
 - [2] G. Yusa, K. Muraki, K. Takashina, K. Hashimoto and Y. Hirayama, *Nature* **434**, 1001 (2005).
 - [3] J. R. Petta, A. C. Johnson, J. M. Taylor, E. A. Laird, A. Yacoby, M. D. Lukin, C. M. Marcus, M. P. Hanson, A. C. Gossard, *Science* **309**, 2180 (2005).
 - [4] D. J. Reilly, J. M. Taylor, J. R. Petta, C. M. Marcus, M. P. Hanson, A. C. Gossard, *Science* **321**, 781 (2008).
 - [5] O. Tsypliyatev and D. Loss, *Phys. Rev. Lett.* **106**, 106803 (2011).
 - [6] G. Kiioseoglou, M. Yasar, C. H. Li, M. Korkusinski, M. Diaz-Avila, A. T. Hanbicki, P. Hawrylak, A. Petrou, and B. T. Jonker, *Phys. Rev. Lett.* **101**, 227203 (2008).
 - [7] M. N. Makhonin, K. V. Kavokin, P. Senellart, A. Lemaitre, A. J. Ramsay, M. S. Skolnick and A. I. Tartakovskii, *Nature Materials* **10**, 844 (2011).
 - [8] E. Baudin, E. Benjamin, A. Lemaitre, and O. Krebs, *Phys. Rev. Lett.* **107**, 197402 (2011).
 - [9] L. Besombes, Y. Leger, L. Maingault, D. Ferrand, and H. Mariette, *Phys. Rev. Lett.* **93**, 207403 (2004).
 - [10] J. Fernández-Rossier and L. Rey, *Phys. Rev. Lett.* **93**, 117201 (2004); J. Fernández-Rossier, *Phys. Rev. B* **73**, 045301 (2006).
 - [11] A. O. Govorov, *Phys. Rev. B* **72**, 075358 (2005).
 - [12] F. Qu and P. Hawrylak, *Phys. Rev. Lett.* **95**, 217206 (2005).
 - [13] Y. Léger, L. Besombes, L. Maingault, D. Ferrand, and H. Mariette, *Phys. Rev. Lett.* **95**, 047403 (2005); Y. Léger,

- L. Besombes, J. Fernández-Rossier, L. Maingault, and H. Mariette, Phys. Rev. Lett. **97**, 107401 (2006).
- [14] F. Qu and P. Hawrylak, Phys. Rev. Lett. **96**, 157201 (2006).
- [15] S.-J. Cheng and P. Hawrylak, Eur. Phys. Lett. **81**, 37005 (2008).
- [16] R. M. Abolfath, P. Hawrylak, I. Zutic, Phys. Rev. Lett. **98**, 207203 (2007); New J. Phys. **9**, 353 (2007).
- [17] R. M. Abolfath, A. Petukhov, I. Zutic, Phys. Rev. Lett. **101**, 207202 (2008).
- [18] C. Le Gall, L. Besombes, H. Boukari, R. Kolodka, J. Cibert, and H. Mariette, Phys. Rev. Lett. **102**, 127402 (2009).
- [19] Nga T.T. Nguyen and F.M. Peeters, Phys. Rev. B **80**, 115335 (2009).
- [20] A. Trojnar, M. Korkusinski, E. Kadantsev, P. Hawrylak, M. Goryca, T. Kazimierzuk, P. Kossacki, P. Wojnar, and M. Potemski, Phys. Rev. Lett. **107**, 207403 (2011).
- [21] R. Oszwaldowski, I. Zutic, A. G. Petukhov, Phys. Rev. Lett. **106**, 177201 (2011).
- [22] S. T. Ochsenbein, Y. Feng, K. M. Whitaker, E. Badaeva, W. K. Liu, X. Li, and D. R. Gamelin, Nature Nanotechnology **4**, 681 (2009).
- [23] G. D. Fuchs, G. Burkard, P. V. Klimov and D. D. Awschalom Nature Physics **7**, 789 (2011).
- [24] B.E. Kane, Nature **393**, 133 (1998).
- [25] H. O. H. Churchill, A. J. Bestwick, J. W. Harlow, F. Kuemmeth, D. Marcos, C. H. Stwertka, S. K. Watson, C. M. Marcus, Nature Physics **5**, 321 (2009).
- [26] *The Physics of Diluted Magnetic Semiconductors*, Springer series in materials science, Springer-Verlag 2011, J. Gaj and J. Kossut, Editors.
- [27] M. A. Ruderman and C. Kittel, Phys. Rev. **96**, 99 (1954).
- [28] Daniel Loss, Fabio L. Pedrocchi, and Anthony J. Leggett Phys. Rev. Lett. **107**, 107201 (2011).
- [29] S. Raymond, S. Studenikin, A. Sachrajda, Z. Wasilewski, S.-J. Cheng, W. Sheng, P. Hawrylak, A. Babinski, M. Potemski, G. Ortner, and M. Bayer, Phys. Rev. Lett. **92**, 187402 (2004).
- [30] J. K. Furdyna, J. Appl. Phys. **64**, R29 (1988).